33rd Annual International Conference of the IEEE EMBS
Boston, Massachusetts USA, August 30 - September 3, 2011

A comparison study of different RF shields for an 8-element transceive small animal array at 9.4T

Jin Jin, Yu Li, Feng Liu, Ewald Weber, and Stuart Crozier, *Member, IEEE*

***Abstract*— In this study, three types of radio-frequency shields are studied and compared in the context of ultra-high field small-animal magnetic resonance imaging. It has been demonstrated that the coil penetration depth and mutual coupling between the coils depend heavily on the type of shield employed. The results were used to guide the design of a 9.4T 8-element transceive small animal array, which provides high overall coil penetration.**

I. Introduction

THIS paper investigates and compares, within the context of ultra-high field (UHF) small-animal imaging, three types of radio-frequency (RF) shields and their effects on the RF penetration and the mutual coupling between neighbouring elements. The results of this study are then applied to the design of an 8-element transceive small animal array coil for a Bruker 9.4T Avance III magnetic resonance imaging (MRI) system.

The promise that the intrinsic signal-to-noise ratio (SNR) of MRI is linearly proportional to the strength of the static magnetic field (B_0), has been driving the research and development towards high fields (HF) and UHF [1, 2]. The higher SNR has the potential to enhance spatial and/or temporal resolution in imaging applications. At higher B_0 and increased Larmor frequencies, however, a number of associated issues have to be addressed. At higher frequencies, the physical dimension of the RF coil becomes comparable to that of the scanned objects. The short electrical wavelengths within the conductive samples cause severe image distortions, exhibited as intensity variations and signal voids [3, 4]. Meanwhile, the local maxima of the electric fields indicate concentrations of energy deposition, which pose a safety concern [3, 5]. "B_1-shimming" [6-8] and parallel transmission techniques [9, 10] have been proposed to tackle the RF magnetic field (B_1) inhomogeneity. These techniques mandate the use of multi-channel transmit array coils and address the issue of B_1 inhomogeneity by manipulating the magnitude and phase of each element in the array. In order for these techniques to work in practice, two aspects of the RF coil design have to be treated carefully, namely coil penetration depth and mutual coupling. These issues are further complicated in designing small-animal

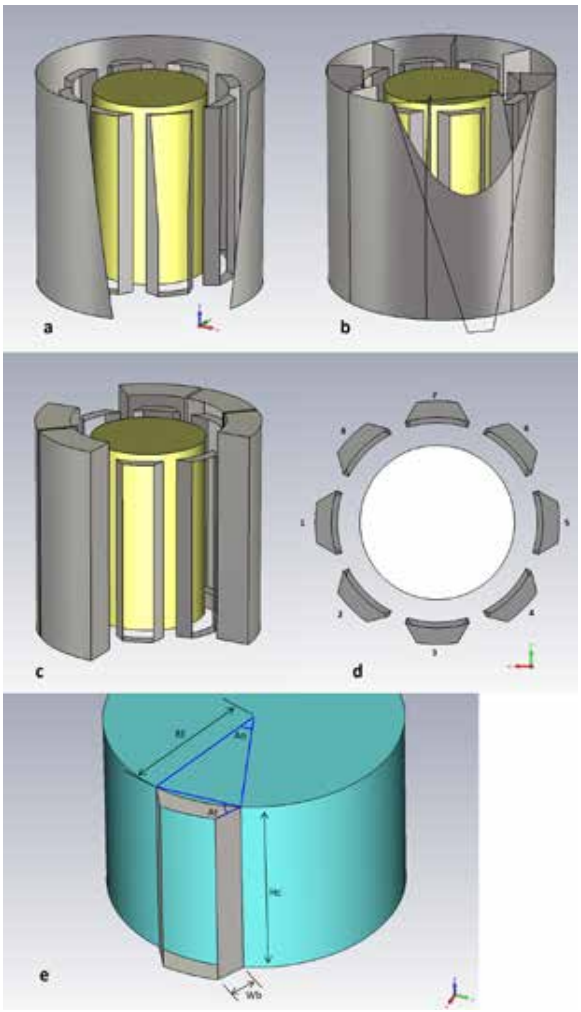

Figure 1 Modelling of RF system with three types of RF shields. (a)-conventional cylindrical shield; (b)-isolation wall shield; (c)-individual shields, which has some of the shields omitted for clarity reasons; (d)-relative positions of coil elements; and (e)-coil structure employed, where A_o=open angle, A_t=tilting angle, W_b=width of blade, R_f=radius of coil former, and H_c=height of coil.

Manuscript received March 25, 2011.

J. Jin, Y. Li, F. Liu, E. Weber and S. Crozier are with the School of Information Technology and Electrical Engineering, the University of Queensland, Queensland 4072, Australia.

Emails: jinjin@itee.uq.edu.au (J. Jin); yuli@itee.uq.edu.au (Y. Li); feng@itee.uq.edu.au (F. Liu); ewald@itee.uq.edu.au (E. Weber) and stuart@itee.uq.edu.au (S. Crozier).

transceive arrays, owing to the strong spatial constraints to accommodate multiple coil elements. Moreover, the techniques [11] introduced to address these issues for human MRI are not readily transferrable to small-animal systems due to the much stronger spatial constraints experienced in the design of small-animal systems. Novel designs have been proposed to circumvent these problems by tailoring the element geometry [12, 13]. The presence of an RF shield however, has significant effects on field penetration and mutual coupling among the elements. Therefore, it is worthwhile investigating the effects of different types of RF shields in the scope of UHF small animal MRI.

In this paper, three types of RF shields, namely a conventional cylindrical shield, an isolation-wall shield [14] and a set of individual shields [15], are investigated for a UHF small-animal system. The effects of the three types of shields on penetration depth and mutual coupling are compared. The findings are then applied to the design of a dedicated 8-channel transceive array.

II. Methods

In this section, the effects of the three aforementioned types of shields are investigated in relation to designing an 8-channel tranceive volume coil for small animal imaging. The first type is the conventional cylindrical shield, which is a metallic cylinder with open ends, surrounding the coil arrays. The second shield is based on the cylindrical shield, to which a metallic rectangular blade is inserted radially between each two adjacent coil elements. The third type provides an individual shield to each coil element. Recent studies have demonstrated the feasibility and effectiveness of using angularly oriented radiating structures for coil elements to increase RF penetration depth as well as regulating mutual coupling [12]. This coil element structure had been adopted in this comparison study. As shown in Fig-1, images (a), (b) and (c) depict the modelling of the RF system enclosed by a conventional cylindrical shield, an isolation-wall shield and a set of individual shields, respectively. To isolate the effects of other variables and study the sole effects from the shields, the coil and phantom setup was identical for all cases. Referring to Fig-1e for coil geometry, the coil element had an open angle of 35.17°; the length of 90 mm; and the width of blades of 8 mm in all three cases. The coils were loaded with a cylindrical phantom of the dimensions as follows: diameter = 43.2 mm and height = 90 mm. The dielectric properties of the phantom were: relative permittivity $\varepsilon_r = 2.72$ and conductivity $\sigma = 0.01\ A/m$. Each element was tuned to 400 MHz and matched to 50 ohm.

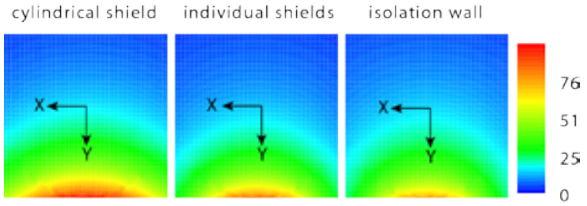

Figure 2 normalized planar RF magnetic fields at z=0 position.

A. 9.4T 8-channel loop-elements transceive array

1) RF Penetration

To evaluate the penetration of each case, a planar magnetic field induced by a single coil element at position 1 was calculated. The calculation was performed in a planar region at z=0 position, ranging from -21.6 mm to 21.6 mm in both x and y axes. The coil elements were driven by one-volt voltage source with zero phases. The magnetic fields were normalized to the source powers in each case. As shown in Fig-2, the shielding has noticeable effects on the corresponding magnetic fields and hence RF penetration depth. The one-dimensional magnetic fields at x=0 positions are compared in Fig-3. At the centre of the phantom (y=0 in Fig.3), the RF magnetic fields were 18.68 A/m for the cylindrical shield, 16.37 A/m for the isolation walls and 15.45 A/m for the individual shields. These values indicate that the cylindrical shield and the isolation walls provide 20.9% and 5.97%, respectively, stronger penetration as compared to that of the individual shields.

2) S-parameters and coupling/decoupling

A second element was then introduced at position 2 (refer to Fig-1d for relative positions of the elements) into each case to study the inherent mutual coupling with no other

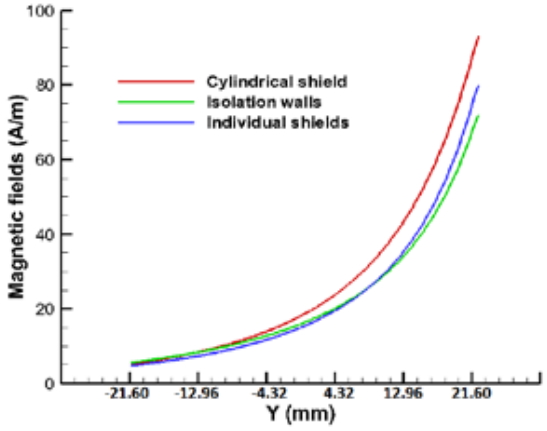

Figure 3 normalized one-dimensional RF magnetic fields at z=x=0 position.

decoupling techniques employed. Two adjacent elements are individually matched and tuned. The absolute S_{11} parameters $|S_{11}|$ are then examined, as shown in Fig-4. The individual shields provide the best channel isolation, depicted as the smallest split of the corresponding $|S_{11}|$; whereas the elements in the cylindrical shield have the strongest mutual coupling. The second coil was then shifted to other positions. The S-parameters were then recorded and summarized in Tab.1. It can be observed that the RF penetration and coil mutual coupling depended heavily on the type of RF shield employed. Among the three types of shields investigated, the conventional cylindrical shield provided the best RF penetration and the least isolation between channels; whereas the individual shields offered the best channel isolation but reduced RF penetration. Meanwhile, isolation walls, as expected, provided a trade-off between the penetration depth and mutual coupling. The isolation-wall shield has metallic plates radially placed between the adjacent coil elements. And unlike the individual shields, the top and the bottom of the structure is not bounded by the metallic shield. The vertical walls of this semi-open structure minimize the effects of leakage flux upon the neighbouring elements, whereas the open ends allow contributions to the magnetic fields inside the region of interests (ROI).

B. 9.4T hybrid loop-sheet 8-channel transceive array

Besides providing shielding to the RF system and isolation among the channels in the array, the isolation walls and individual shields offer great design flexibilities, in that the elements can be of arbitrary shape, size, location and even resonance frequency [15]. In the previous section, the open angle of each coil element was restricted to 35.17° due to the space constraints. To further enhance the penetration of the array, an innovative design is needed to increase the open angle, since the RF penetration is normally proportional to the size of the element.

TABLE 1
S-PARAMETERS OF TWO ELEMENTS AT DIFFERENT RELATIVE POSITIONS

	|S21|	|S31|	|S41|	|S51|
cylindrical shield	2.9 dB	22.8 dB	31.9 dB	34.1 dB
isolation walls	16.7 dB	30.9 dB	33.7 dB	34.4 dB
individual shields	19.3 dB	38.0 dB	41.5 dB	42.1 dB

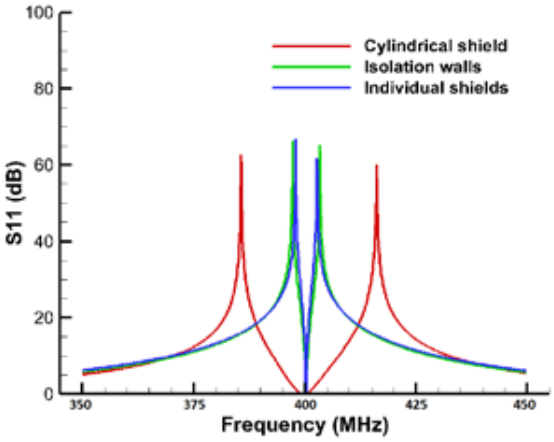

Figure 4 |S11| when a second element is introduced at position 2

In this section, a novel design of RF array is proposed for small-animal imaging at 9.4T. The proposed coil array utilised an interleaved loop-sheet structure. The current sheet antenna (CSA) has been used previously by other researchers in multi-element transceive arrays [16, 17]. In this study, the CSA elements were used to replace some of the loop elements to alleviate the space constraints encountered in designing the small-animal volume coil. The proposed array structure is shown in Fig.5. As can be seen, the CSA elements are less space-consuming, which offers higher degrees of freedom to optimize the loop elements for increased RF penetration. The use of an isolation-wall RF shield enabled the combination of the two types of coil elements, concurrently providing better mutual decoupling.

In the proposed array, the open angle of the loop elements was increased to 45° to accommodate four loop

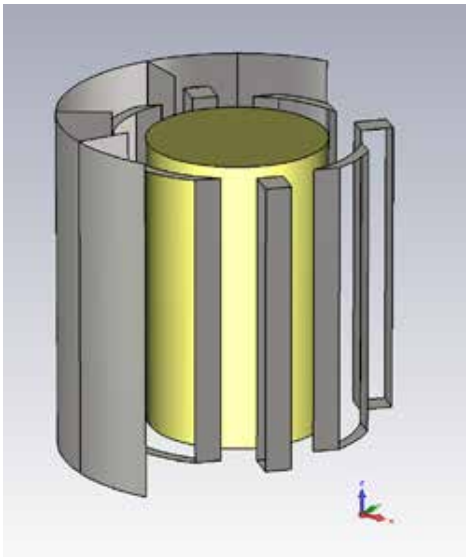

Figure 5 The proposed interleaved loop-sheet coil array. A portion of the shield was removed for clarity reasons.

elements and four CSA elements. The tilting angle of the radiating blades of the new loop coils was optimized. It was shown that 20° tilting angle gave the loop elements the best penetration. The cylindrical phantom, the same as used in section A, had been adopted for loading purpose. Each element was tuned to 400MHz and matched to 50 ohm.

Fig.6 depicts the one-dimensional RF fields calculated at z=x=0 position, to compare the RF penetration of the proposed hybrid structure to the conventional structure as discussed in section A (loop element of 35.17° open angle with cylindrical shield). At the centre of the phantom (x=y=z=0), the RF fields read 24.56 A/m for the hybrid loop element, 18.68 A/m for the hybrid CSA element and 15.28 A/m for the original loop element. By adopting the hybrid array structure, the RF penetration of the enlarged loop elements had seen an increase of 31.4%, which outweighs the decrease (approximately 12.2%) of that in the CSA elements in two respects. First, the percentage increase of RF penetration of the loop elements exceeds the percentage decline of that of the CSA elements. Second, the loop element in the hybrid array accounts for the coverage of most of the ROI. The isolation between adjacent loop element and CSA was 22dB with the isolation-wall shield.

III. Discussion and Conclusion

In this study, three types of RF shields have been investigated in the context of designing volume coils for UHF small animal MRI. The effects of the shields on the RF penetration and mutual coupling were examined in an 8-element transceive array. It was found that the conventional cylindrical shield provided the highest RF penetration but the least mutual decoupling among the elements. The individual shields provide the best isolation among channels at the cost of lowest RF penetration; whereas isolation-wall shields offered a tradeoff between the two. They provided powerful isolation among the coil elements, allowing each element to operate independently within the chambers. The isolation-wall RF shield encouraged the hybrid loop-sheet design of multi-element volume coils. It offered a way to combine the two structures and to take advantage of the beneficial tradeoffs between them.

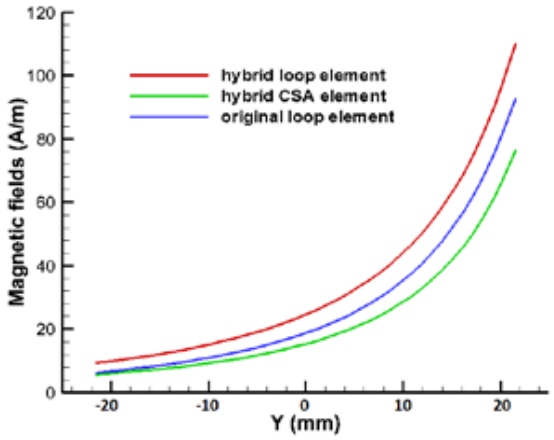

Figure 6 one-dimensional RF fields at z=x=0 position.

References

[1] W. A. Edelstein, *et al.*, "The intrinsic signal-to-noise ratio in NMR imaging," *Magnetic Resonance in Medicine,* vol. 3, pp. 604-618, Aug 1986.

[2] J. T. Vaughan, *et al.*, "7T vs. 4T: RF power, homogeneity, and signal-to-noise comparison in head images," *Magnetic Resonance in Medicine,* vol. 46, pp. 24-30, 2001.

[3] F. Liu, *et al.*, "Numerical modeling of 11.1T MRI of a human head using a MoM/FDTD method," *Concepts in Magnetic Resonance Part B: Magnetic Resonance Engineering,* vol. 24B, pp. 28-38, 2005.

[4] F. Liu and S. Crozier, "Electromagnetic fields inside a lossy, multilayered spherical head phantom excited by MRI coils: models and methods," *Physics in Medicine and Biology,* vol. 49, pp. 1835-1851, May 2004.

[5] B. L. Beck, *et al.*, "Observation of significant signal voids in images of large biological samples at 11.1 T," *Magnetic Resonance in Medicine,* vol. 51, pp. 1103-1107, 2004.

[6] C. M. Collins, *et al.*, "Combination of optimized transmit arrays and some receive array reconstruction methods can yield homogeneous images at very high frequencies," *Magnetic Resonance in Medicine,* vol. 54, pp. 1327-1332, 2005.

[7] T. S. Ibrahim, "Ultrahigh-field MRI whole-slice and localized RF field excitations using the same RF transmit array," *Medical Imaging, IEEE Transactions on,* vol. 25, pp. 1341-1347, 2006.

[8] B. van den Bergen, *et al.*, "SAR and power implications of different RF shimming strategies in the pelvis for 7T MRI," *Journal of Magnetic Resonance Imaging,* vol. 30, pp. 194-202, 2009.

[9] U. Katscher, *et al.*, "Transmit SENSE," *Magnetic Resonance in Medicine,* vol. 49, pp. 144-150, Jan 2003.

[10] Y. Zhu, "Parallel excitation with an array of transmit coils," *Magnetic Resonance in Medicine,* vol. 51, pp. 775-784, 2004.

[11] J. Jevtic, *et al.*, "Design guidelines for the capacitive decoupling networks," in *Proceedings of the 11th Annual Meeting of ISMRM*, 2003, p. 428.

[12] E. Weber, *et al.*, "A Novel 8-Channel Transceive Volume-Array for a 9.4 T Animal Scanner," 2010, pp. 151-151.

[13] Y. Li, *et al.*, "A Stripline-Like Coil Element Structure for High Field Phased Array Coils and Its Application for a 8-Channel 9.4T Small Animal Transceive Array," in *ISMRM*, Stockholm, Sweden, 2010.

[14] Y. Li, *et al.*, "Modelling Study of a Hybrid Loop-Sheet Coil Structure for a 8-channel Small Animal Transceive Array at 9.4T," in *ISMRM*, Montreal, Quebec, Canada, 2011, p. 4686.

[15] K. Gilbert, *et al.*, "Transmit/receive radiofrequency coil with individually shielded elements," *Magnetic resonance in medicine: official journal of the Society of Magnetic Resonance in Medicine/Society of Magnetic Resonance in Medicine,* 2010.

[16] S. Junge, *et al.*, "Current Sheet antenna array-a transmit/receive surface coil array for MRI at high fields," 2004, p. 41.

[17] P. Ullmann, *et al.*, "Experimental analysis of parallel excitation using dedicated coil setups and simultaneous RF transmission on multiple channels," *Magnetic Resonance in Medicine,* vol. 54, pp. 994-1001, 2005.